ÉCOLE POLYTECHNIQUE
FÉDÉRALE DE LAUSANNE

02/03/2018

ME-301 TECHNIQUES DE MESURE

Mesures de vitesse par particle image velocimetry

K. Mulleners

Measuring flow velocities
Ideas, requirements, pro and cons?

PIV Examples

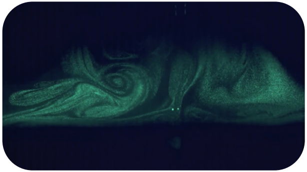

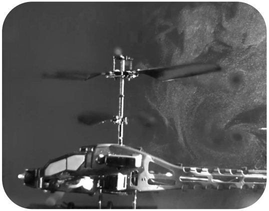

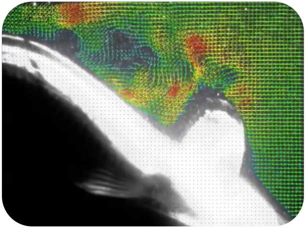

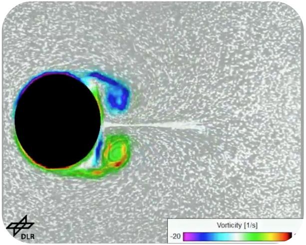

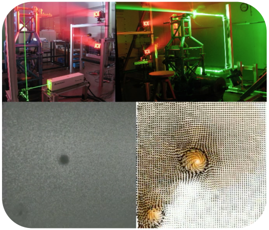

Overview

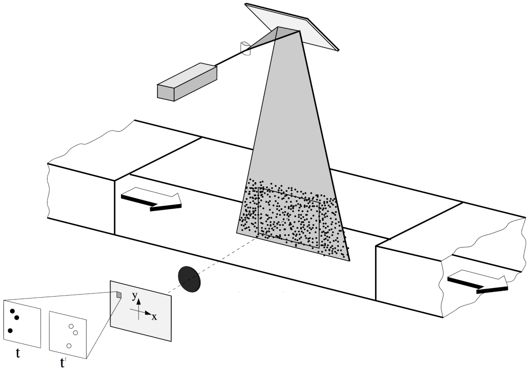

References

M. Raffel, C. Willert. S. Wereley, and J. Kompenhans
Particle Image Velocimetry - A practical guide.
Springer Berlin Heidelberg, 2007.
http://www.springer.com/de/book/9783662491621

C. Tropea, A.L. Yarin, and J.F. Foss
Springer Handbook of Experimental Fluid Mechanics.
Springer Berlin Heidelberg, 2007.
http://link.springer.com/book/10.1007%2F978-3-540-72308-0

PIV principle

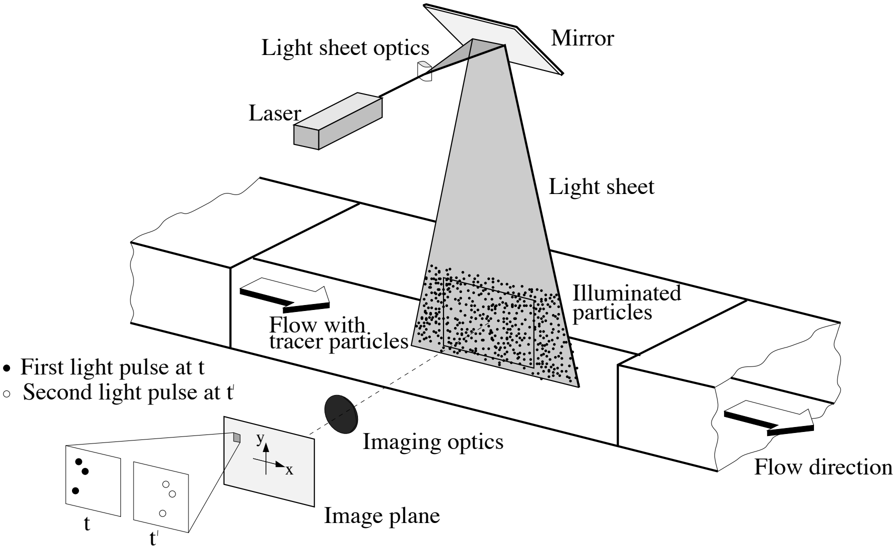

PIV principle

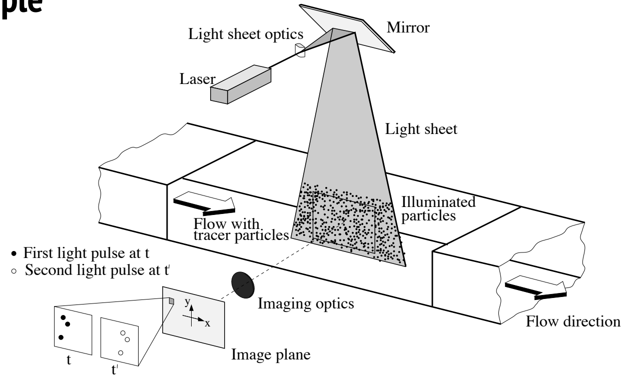

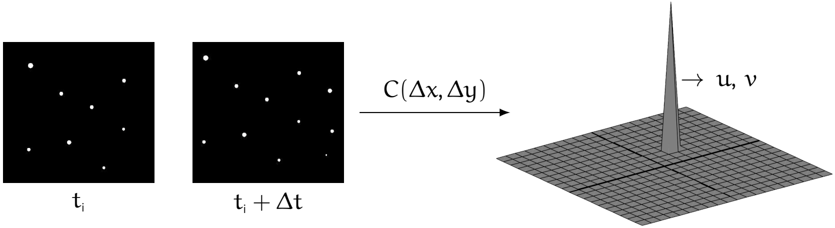

PIV family

Method	Probe Volume [mm³]
a) Stereo-PIV $f = 10$ Hz, Area = 40 x 40 cm²	5 x 5 x 1
b) High-Speed Stereo-PIV $f = 1$ kHz, Area = 10 x 10 cm²	5 x 5 x 1
c) Multi-plane Stereo-PIV $f = 10$ Hz, Area = 40 x 40 cm², variable Δt, Δz	5 x 5 x Δz
d) Photographic holographic PIV $f = 0$ Hz, Volume = 5 x 5 x 5 cm³	1 x 1 x 1
e) Digital holographic PIV $f = 10$ Hz, Volume = 1 x 1 x 1 cm³	1 x 1 x 1
f) Tomographic PIV $f = 10$ Hz, Volume = 6 x 6 x 1.5 cm³	2 x 2 x 1
g) High-speed Tomographic PIV $f = 1$ kHz, Volume = 3 x 3 x 1 cm³	2 x 2 x 1

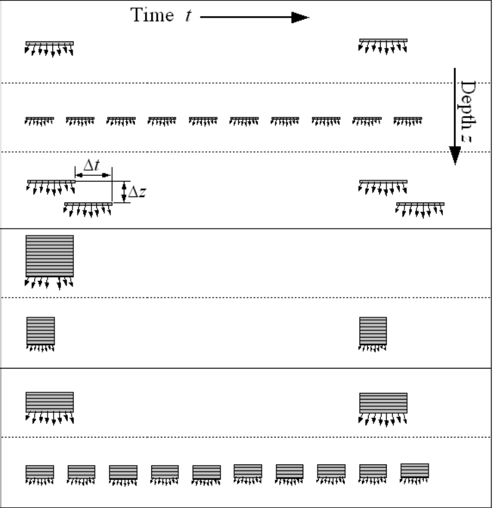

Tracer particles

The PIV technique is indirect, it determines the particle velocity instead of the fluid velocity
$\Rightarrow$ special care is required to select suitable seeding particles to avoid discrepancies between fluid and particle motion

A primary source of error = mismatch between the densities of the fluid ρ and the tracer particles ρ_p

Gravitationally induced velocity of spherical particles acceleration (assuming Stokes' flow)

$$\vec{U}_g = d_p^2 \, \frac{(\rho_p - \rho)}{18\mu} \, \vec{g}$$

$\Rightarrow$ velocity lag of a particle in a continuously accelerating fluid:

$$\vec{U}_s = \vec{U}_p - \vec{U} = d_p^2 \, \frac{(\rho_p - \rho)}{18\mu} \, \vec{a}$$

$\vec{g}$	the acceleration due to gravity
μ	dynamic fluid viscosity
d_p	particle diameter
$\vec{U}_p$	particle velocity

Light scattering behaviour

$d_p = 1\,\mu s$

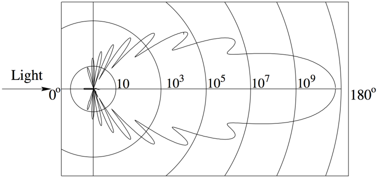

Light scattered by small spherical particles ($d_p > \lambda$)
= Mie scattering

$d_p = 10\,\mu s$

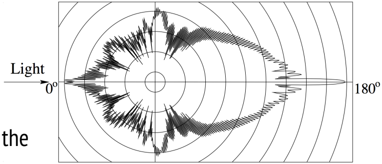

Intensity of light scattered a function of:

- the particles' size, shape and orientation
- the ratio of the refractive index of the particles to that of the surrounding medium
- polarisation of the light
- observation angle

$d_p = 30\,\mu s$

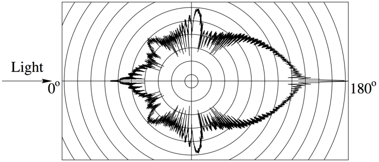

Seeding in liquid flows

Type	Material	Mean diameter in µm
Solid	Polystyrene	10 – 100
	Aluminum flakes	2 – 7
	Hollow glass spheres	10 – 100
	Granules for synthetic coatings	10 – 500
Liquid	Different oils	50 – 500
Gaseous	Oxygen bubbles	50 – 1000

Additional advantage for solid particles: fluorescent coating

Seeding in liquid flows

Fluorescent particles

A simple and inexpensive way of producing your own fluorescent seeding particles

A. Müller, M. Dreyer, A. Favrel, N. Andreini, P. Bouillot, M. Farhat and F. Avellan
EPFL Laboratory for Hydraulic Machines, 1007 Lausanne, Switzerland

Context and problem

High fluid volumes in test rigs for hydraulic machinery

- Reduced scale models of hydraulic turbines > **30 m^3**
- Cavitation tunnels > **100 m^3**

High cost of commercially available fluorescent seeding material

- Typically **> USD 2,500** for **100 g** of fluorescent polymer particles (FPP)

✓ **Self-made** fluorescent polyamide seeding particles (FPSP)

✓ Based on off-the-shelf PSP and Rhodamine dye.
✓ Limited one-time invest. and small running costs.

✓ Excellent optical properties and longevity.
✓ Cost reduction of up to 45 times for seeding.

Example of application

Cavitation effect on a tip vortex measured in a cavitation tunnel [2]

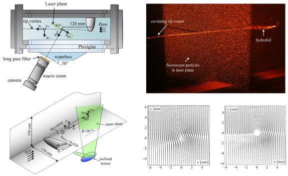

Instructions for particle preparation and filtering

Ingredients

- Off-the-shelf PSP
- Rhodamine Dye (B or 6G)

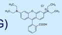

Shopping list

- Incubator
- Polyamide particles
- Rhodamine dye (RhB or Rh6G)
- Methanol
- Büchner funnel and rubber seal
- 4-12 μm filter paper
- Glass flask
- Water aspirator (vacuum pump)

Instructions[1]

- Regularly agitate while in incubator
- Take out after 4-8 weeks at 60°C
- Rinse with water over filter paper
- Remove, stir in methanol bath for under 1 minute, change filter paper
- Rinse with water again until clear
- Read Rhodamine safety sheet

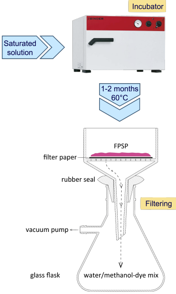

11TH INTERNATIONAL SYMPOSIUM ON PARTICLE IMAGE VELOCIMETRY – PIV15
Santa Barbara, California, September 14-16, 2015

Poster 276
andres.mueller@epfl.ch

Seeding in gas flows

Type	Material	Mean diameter in µm
Solid	Polystyrene	0.5 – 10
	Alumina Al_2O_3	0.2 – 5
	Titania TiO_2	0.1 – 5
	Glass micro-spheres	0.2 – 3
	Glass micro-balloons	30 – 100
	Granules for synthetic coatings	10 – 50
	Dioctylphathalate	1 – 10
	Smoke	$<$ 1
Liquid	Different oils	0.5 – 10
	Di-ethyl-hexyl-sebacate (DEHS)	0.5 – 1.5
	Helium-filled soap bubbles	1000 – 3000

Light sources

Laser   light amplification by stimulated emission of radiation

Neodym-YAG lasers (Nd:YAG lasers $\lambda = 1064$nm and $\lambda = 532$nm) are the most important solid-state laser for PIV in which the beam is generated by Nd^{3+} ions.

Properties and specifications of modern Nd:YAG PIV-laser systems

Repetition rate	10Hz
Pulse energy for each of two pulses	320mJ
Roundness at 8m from laser output	75%
Roundness at 0.5m from laser output	75%
Spatial intensity distribution at 8m from laser output	$<$ 0.2
Spatial intensity distribution at 0.5m from laser output	$<$ 0.2
Linewidth	1.41 / cm
Power drift over 8 hours	$<$ 5%
Energy stability	$<$ 5%
Beam pointing stability	100 µrad
Deviation from collinearity of laser beams	$<$ 0.1 mm / m
Beam diameter at laser output	9 mm
Divergence	0.5 mrad
Jitter between two following laser pulses	2ns
Delay between two laser pulses	0 to 10ms
Resolution	5 ps
Working temperatures	15°-35°C
Cooling water	10°C - 25°C
Power requirements	220–240 V , 50 Hz

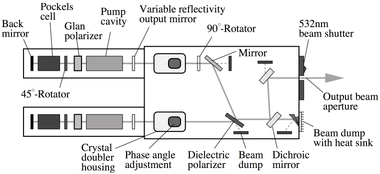

Light sources

Laser light amplification by stimulated emission of radiation

Neodym-YLF lasers (Nd:YLF lasers $\lambda = 1053$ nm and $\lambda = 526$ nm) are used for an increasing number of applications, including high repetition rate PIV techniques, which require a reliable high average-power laser source that enables efficient frequency conversion to visible wavelengths.

Properties and specifications of a high repetition rate Nd:YLF PIV-laser system

Repetition rate	0.01 kHz to 10 kHz
Pulse energy for each of two pulses	15 mJ to 3 mJ
Roundness at 4 m from laser output	75%
Roundness at 0.5 m from laser output	75%
Spatial intensity distribution at S I 4m from laser output	$<$ 0.2
Spatial intensity distribution at 0.5 m from laser output	$<$ 0.2
Pulse width at S I 1kHz	$<$ S I 180ns
Power drift over 8 hours	$<$ 5%
Energy stability	$<$ 1%
Deviation from co-linearity of laser beams	$<$ 0.1 mm / m
Beam diameter at laser output	2 mm
Divergence	$<$ 3 mrad
Spatial mode	multi-mode, $M^2 < 6$
Cooling water	10° – 25° C

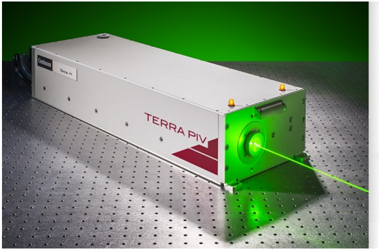

Light sources
LED light-emitting diode

LED head specifications	
Pulses	0 A to 200 A
Power	0 mW^2/cm to 47 mW^2/cm
Colours	green, blue, red, white, UV

Controller specifications	
Resolution	5 ns
Jitter	ultra low
Pulses	TTL
Repetition rate	0.047 Hz to 2500 Hz
Trigger inputs	3; 0.047 MHz to 2 MHz
Trigger logic	AND, OR, INVERT
Trigger delay	user definable
Trigger window	user definable
Operating modes	incremental encoder mode, double pulse PIV-mode, CW-mode
PC connection	100 Mbit Ethernet
Channels	up to 2 LED-heads
Supply	110 V to 230 Vac, 25 Hz to 30 Hz

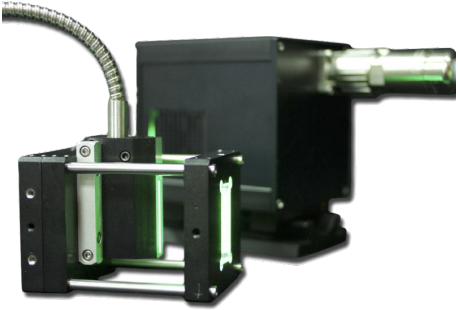

Image recording
Cameras

charge coupled devices CCD complementary metal-oxide-semiconductor CMOS

moves charge from pixel to pixel and convert it to voltage at output node

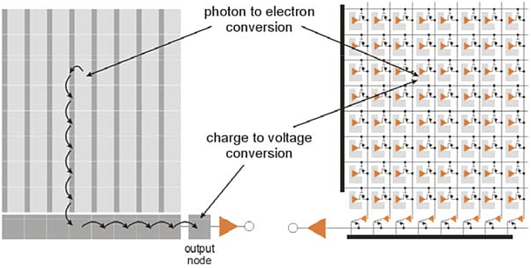

converts charge to voltage inside one pixel

- CCD cameras are more sensitive at 550nm (approx. factor 2)
- CCD cameras show lower dark noise (factor 5-10)
- CCD sensors show less inhomogeneous sensitivity (<0.5 % vs 1.5 % for CMOS)
- CCD cameras show less artefacts in the images (higher production tolerances)
- CMOS cameras are much faster (parallel readout)
- CMOS cameras don’t show blooming effects

Image recording
Technical data camera

image sensor

type of sensor	CCD
image sensor	ICX285AL
resolution (h x v)	1392 x 1040 pixel (normal)
	800 x 600 pixel (center ROI)
pixel size (h x v)	6.45 µm x 6.45 µm
sensor format / diagonal	2/3" / 11.14 mm
shutter mode	global (snapshot)
MTF	77.5 lp/mm (theoretical)
fullwell capacity	16 000 e^-
	24 000 e^- (binning)
readout noise	5 .. 7 e^- rms @ 12 MHz (typ.)
	6 .. 8 e^- rms @ 24 MHz (typ.)
dynamic range	2 667 : 1 (68 dB)
	4 000 : 1 (72 dB, binning)
quantum efficiency	62 % @ peak
spectral range	290 nm .. 1100 nm
dark current	1 e^-/pixel/s @ 23 °C
DSNU[1]	2 e^- rms
PRNU[2]	< 1 %

camera

max. frame rate	7.3 / 13.5 fps (12 / 24 MHz, normal)
	11.7 / 21.6 fps (12 / 24 MHz, center)
exposure/shutter time	1 µs .. 60 s
dynamic range A/D	14 bit
A/D conversion factor	1.0 e^-/count
	1.5 e^-/count
pixel scan rate	12 MHz / 24 MHz
pixel data rate	19.5 Mpixel/s
binning (hor x ver)	1 x 1 .. 4 x 4
non linearity	< 1 %
smear	< 0.002 %
anti-blooming factor	> 400 (standard 100 ms exposure)
	> 4 (NIR boost 100 ms exposure)
interframing time[3]	1 µs (optional)
trigger input signals	software / TTL level
trigger output signals	3.3 V LVTTL level
data interface	USB 2.0

general

power supply	9 .. 28 VDC (12 VDC typ.)
power consumption	< 4 W
weight	0.25 kg
operating temperature	+ 10 °C .. + 45 °C
operating humidity range	10 % .. 80 % (non-condensing)
storage temperature range	- 20 °C .. + 70 °C
optical interface	C-mount
CE certified	yes

frame rate table

resolution	normal		center	
pixelclock [MHz]	12	24	12	24
1392 x 1040	7.3 fps	13.5 fps		
800 x 600			11.7 fps	21.6 fps
v2 binning	14.7 fps	27.0 fps	21.8 fps	40.4 fps
v4 binning	27.0 fps	47.0 fps	35.0 fps	62.0 fps

quantum efficiency

monochrome

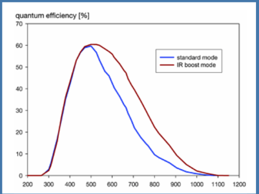

f/2.8

more light

f/16

smaller depth of focus

1 dark signal non-uniformity measured in a 90% center zone of the image sensor
2 photo response non-uniformity
3 time between two consecutive images for particle image velocimetry (PIV) applications

Image recording

Stereo PIV

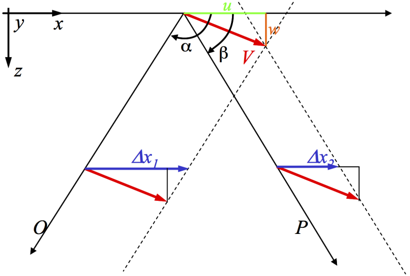

$$\begin{bmatrix} \Delta x_1 \\ \Delta y_1 \\ \Delta x_2 \\ \Delta y_2 \end{bmatrix} = \begin{bmatrix} 1 & 0 & -\frac{O_x}{O_z} \\ 0 & 1 & -\frac{O_y}{O_z} \\ 1 & 0 & -\frac{P_x}{P_z} \\ 0 & 1 & -\frac{P_y}{P_z} \end{bmatrix} \cdot \begin{bmatrix} u \\ v \\ w \end{bmatrix}$$

$$\Delta\vec{X} = \mathbf{A} \cdot \vec{V}$$

$$\vec{V} = (\mathbf{A}^T \mathbf{A})^{-1} \mathbf{A}^T \Delta\vec{X}$$

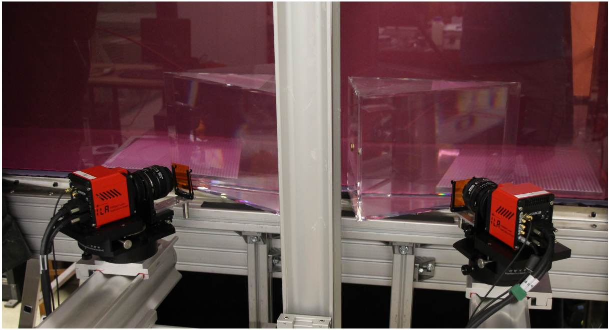

Image recording

Stereo PIV

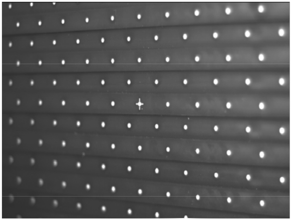

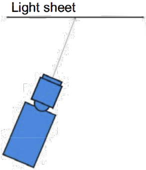

Only vertical line in the center is focussed.

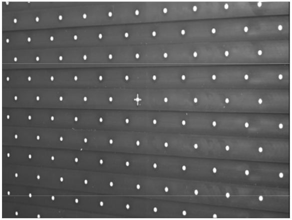

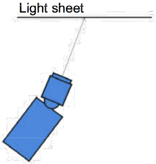

Complete FOV is focussed.

Scheimpflug principle

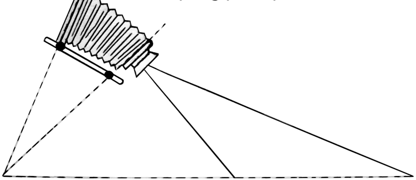

Timing schemes for PIV recording

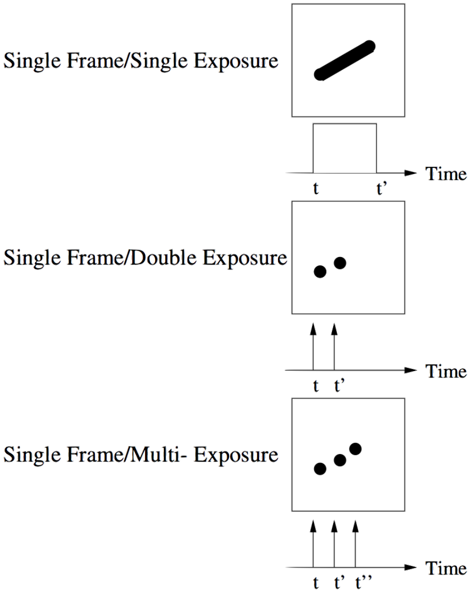

Timing schemes for PIV recording

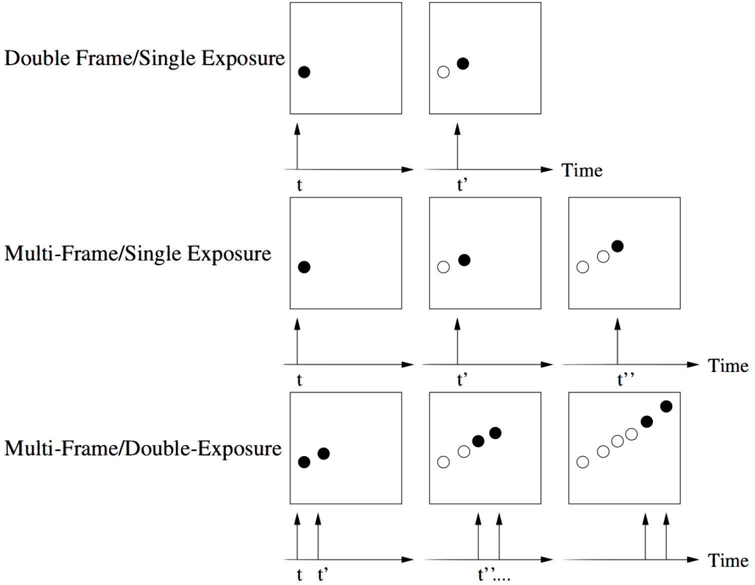

Timing and synchronisation of illumination and imaging

Frame-straddling mode

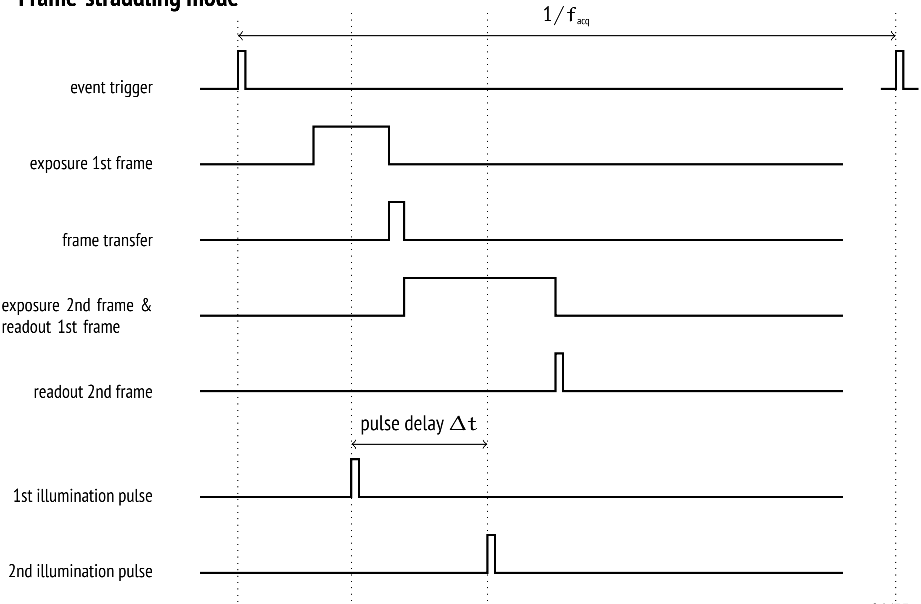

Calibration

Why?

- determine the imaging magnification factor M
- correct for lens distortions
- stereo mapping

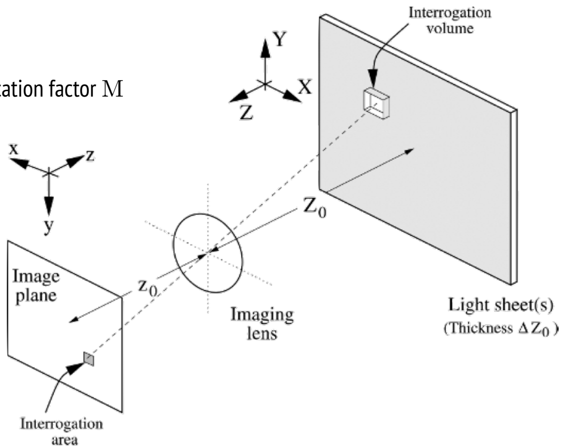

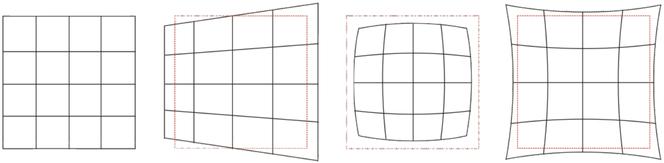

Calibration $u = \frac{\Delta x}{M}\frac{1}{\Delta t}$, $[\Delta x] = \mathrm{px}$, $[\Delta t] = \mathrm{s}$

M =... px/mm

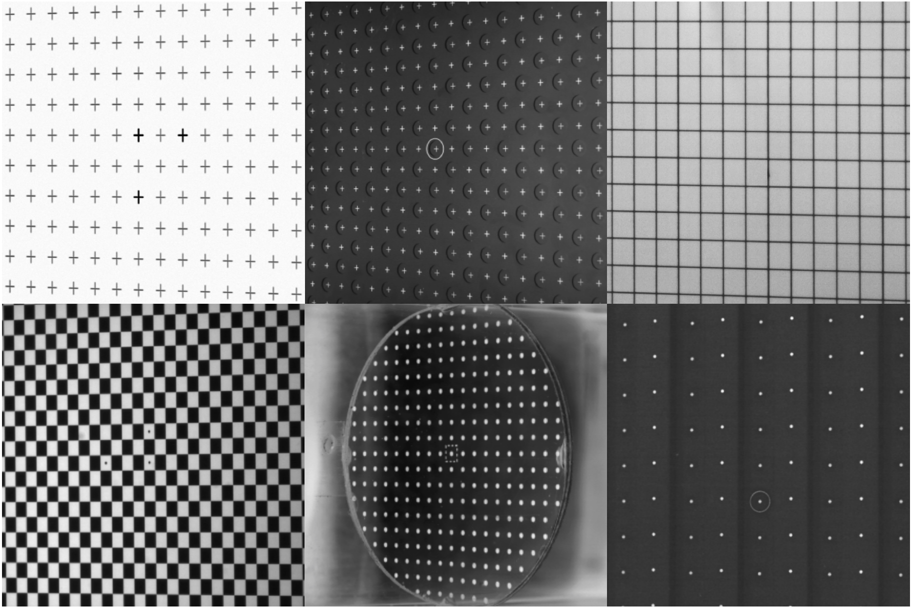

Cross-correlation

cross-correlation via
digital Fourier transform

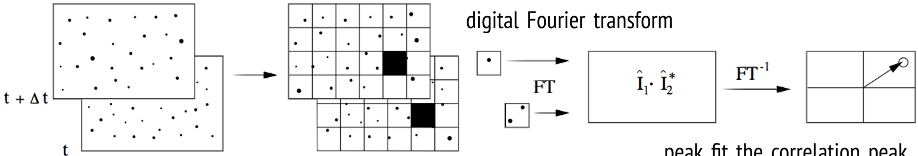

divide in interrogation windows

peak fit the correlation peak
to obtain displacement in px

cross-correlation plane $R(\Delta x, \Delta y)$

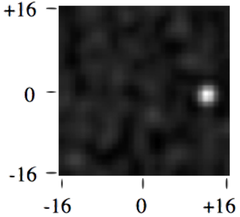

Measurement noise and accuracy

The overall measurement accuracy in PIV is a combination of a variety of aspects extending from the recording process all the way to the methods of evaluation.

The absolute measurement error in the estimation of a single displacement vector ϵ_{tot} can be decomposed into a group of **systematic errors**, ϵ_{sys} and a group of **residual errors** ϵ_{res}:

$$\epsilon_{\text{tot}} = \epsilon_{\text{sys}} + \epsilon_{\text{res}}$$

The systematic errors comprise all errors which arise due to the inadequacy of the statistical method of cross-correlation in the evaluation of a PIV recording, such as its application in gradient regions or the use of an inappropriate sub pixel peak estimator. The nature of these errors is that they follow a consistent trend which makes them predictable. By choosing a different analysis method or modifying an existing one to suit the specific PIV recording, the systematic errors can be reduced or even removed.

The second type of errors, the residual errors, remain in the form of a measurement uncertainty even when all systematic errors have been removed. In practice, it is not always possible to completely separate the systematic errors from the residual errors such that we choose to express the total error as the sum of a **bias error** ϵ_{bias} and a **random error** or measurement uncertainty, ϵ_{rms}:

$$\epsilon_{\text{tot}} = \epsilon_{\text{bias}} + \epsilon_{\text{rms}}$$

Measurement noise and accuracy

Each displacement vector is thus associated with a certain degree of over or under estimation, hence a bias error ϵ_{bias}, and some degree of random error or measurement uncertainty $\pm\epsilon_{\text{rms}}$

$$\epsilon_{\text{tot}} = \epsilon_{\text{bias}} + \epsilon_{\text{rms}}$$

The **random error** refers to measurement uncertainties induced and affected by the particle image diameter, the size of the interrogation window size, and the particular flow conditions (e.g. strong shear, rotation, etc.).

The interrogation windows size has an important influence on the measurement uncertainty which increases with decreasing interrogation window size. Selecting a final interrogation window size is finding a compromise between a high spatial resolution and a low random error.

The **bias error** is mainly determined by peak locking, a phenomenon describing the tendency of the displacements to be biased toward integer pixel values

Interrogation window size
Making the right choice

choice depends on:

- flow
- seeding
- imaging
- timing

too small interrogation window size

→ not enough particles in interrogation window

→ particles 'leave' interrogation window

too large interrogation window size

→ decreased spatial resolution

→ multiple correlation peaks

⇒ **one choice does not fit all**

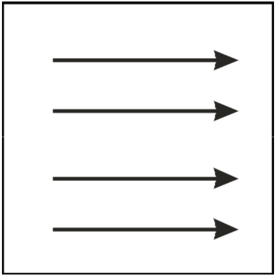

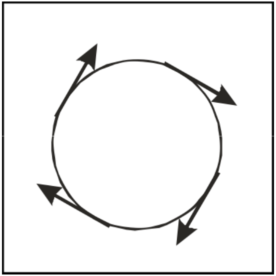

Milti-grid processing

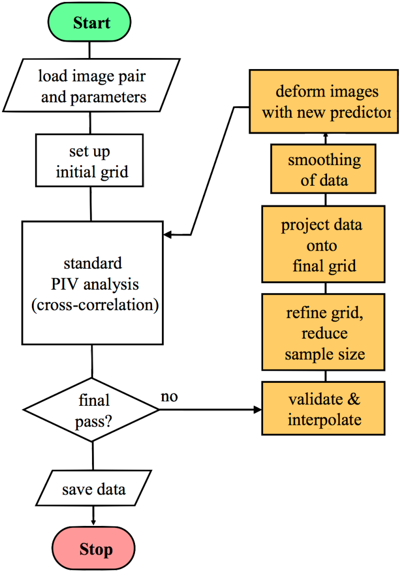

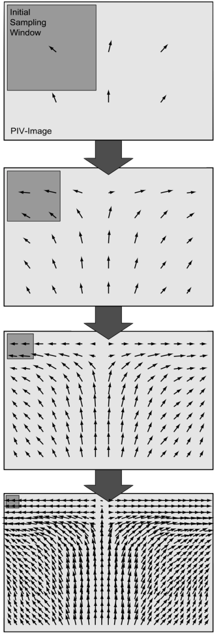

Peak fitting and peak locking

Particle image

Correlation Map (in x-direction)

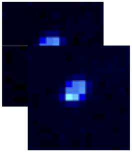

Partial overlap :

Broad peak →
gaussian bell fit →
Subpixel accuracy

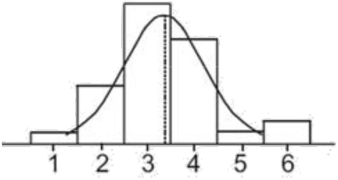

particle image size of 2-3 pixel

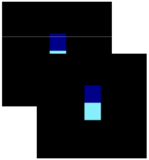

Overlap or not :

Single peak →
gaussian bell fit →
Pixel accuracy

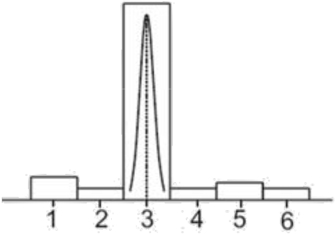

particle image size smaller than 1 pixel

TP setup

- water channel with variable speed
- LED illumination
- 14bit CCD camera 1392 px $\times$ 1040 px
- Synchroniser
- PIVlab

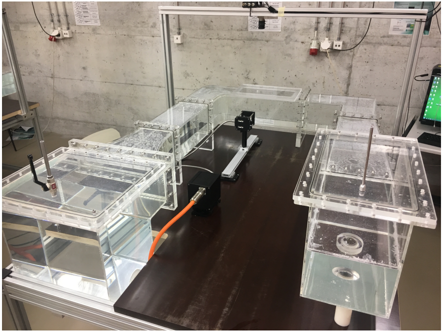

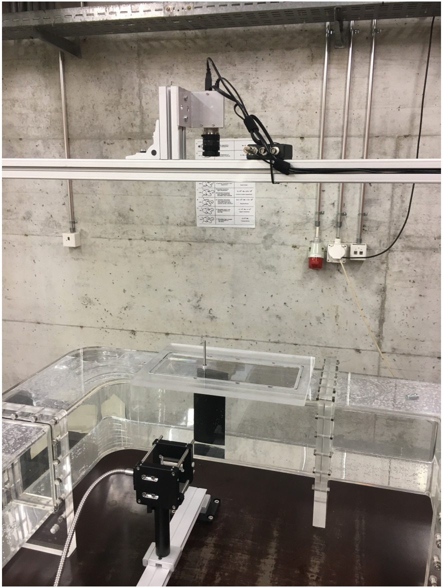

TP setup

Compare the wakes of different cars